JOURNAL OF COMPUTATIONAL PHYSICS 83, 79–95 (1989)

An Efficient Scheme for Convection-Dominated Transport

W. N. G. HITCHON, D. J. KOCH, AND J. B. ADAMS

Department of Electrical and Computer Engineering, University of Wisconsin-Madison Madison, Wisconsin 53706

Received January 25, 1988; revised August 23, 1988

Partial differential equations describing transport processes involving a significant effect of the flow velocity may be solved efficiently and easily, using a simple algorithm. The algorithm is based on the propagator(s) (or Green's functions) for the equations of transport theory. The numerical method employed is always at least as fast as finite differencing, and it reduces to a finite difference method in the short time-step limit, but is especially efficient in cases where flow dominates over diffusion and is consequently widely applicable in kinetic theory and fluid dynamics. Using this method, the ion distribution function and the potential in a plasma sheath were calculated in the presence of charge exchange collisions for a wide range of neutral densities. © 1989 Academic Press, Inc.

I. INTRODUCTION

The numerical solution of the partial differential equations which describe the transport of fluids is usually accomplished by means of finite difference schemes [1–3]. For many such problems the finite-difference method is computationally expensive due to limitations placed on the time-step by the nature of finite differencing (the Courant–Friedrichs–Levy (CFL) criterion). In this paper, we present a method which completely removes the CFL limit for an important class of problems.

To be more specific, the CFL limit arises because the various derivatives of the "density" n at a mesh point labelled i are usually evaluated in terms of the values of the density at the neighboring points, labelled $i \pm 1$. As a result, in advancing the solution at i through one time-step using an explicit scheme, the only information available as to the density elsewhere concerns conditions one mesh-space away from the point i. This in turn means that the rate of propagation of information across the numerical mesh is limited to one mesh-spacing, Δx, per time-step Δt. If the physical propagation rate exceeds this we have at best inaccuracy and at worst instability.

To see why this limit is so restrictive, consider a problem in kinetic theory where we need to find the density in the phase space (x, v_x). The mesh is now labelled by indices (i, j), corresponding to the values of x and v_x, respectively. For simplicity we momentarily neglect the forces on the fluid, including collisions. Then $\dot{v}_x = 0$,

581/83/1-6

0021-9991/89 $3.00

and the problem is simply one of describing the fluid density evolving subject to the flow, with $\dot{x} \equiv v_x$.

If this problem is solved using finite differences, the fastest moving particles, having velocity $\pm v_{\max}$, provide the most stringent limit on the time-step, since the time-step must be chosen so that even they do not travel Δx in time Δt. In principle, then, $\Delta t < \Delta t_{\text{CFL}} = \Delta x / v_{\max}$. The slowest moving particles require many such time-steps to move a significant distance.

There is no fundamental reason why Δt must be so small. In earlier work [4] we treated a problem of the nucleation and growth of thin films using the propagator, Eq. (A3), in one dimension (the cluster size). The solutions were compared to those obtained from an exact propagator we found for the set of difference equations governing cluster growth. It was pointed out that the propagator was still valid when $\delta x > \Delta x$, i.e., clusters grow by more than one atom per time step. This is by contrast with the conclusions of a previous study [5] of void growth in irradiated metals, which used the same propagator in one dimension, but implemented it differently and so obtained limits on the time step equivalent to the CFL criterion.

The purpose of this paper is to present an approach to overcome the limitation which the flow velocity imposes on Δt. Implicit finite difference schemes go some way to overcome this problem, in that they do not normally go unstable, and so large steps may be used if accuracy can be sacrificed, which is sometimes acceptable if only the steady-state solution is needed. In general, however, they are subject to similar limitations as explicit schemes, if the time evolution of the system is of interest. This method is also much easier to use than an implicit scheme.

In the next section we shall describe our method in detail. In Section III, we apply it to description of a plasma sheath, and in Section IV, we summarise the method.

II. The Numerical Scheme

In this section, we develop the method to be used in this work. We begin with the simple example mentioned above where the only transport process is a flow with a constant velocity. Collisions are then added. In the next subsection we extend this to a more realistic flow involving variable velocities and collisions. We then describe the boundary conditions used, and finally we discuss the method in the context of other methods.

A. *Description of Simplified Numerical Method*

In the kinetic problem considered above (and with $\dot{v}_x = 0$ still) we first decide on a time-step Δt which is appropriate on physical or numerical grounds other than the CFL criterion. The basis for this choice will be discussed presently, but we envisage that $\Delta t \gg \Delta t_{\text{CFL}}$ in our example. Particles in some representative cell will travel a distance $\delta x = v_x \Delta t$ in this time, and the distance can be much greater than the mesh spacing; $\delta x \gg \Delta x$. When the number of cells crossed is an integer,

$\delta x/\Delta x = \delta i$, then the density $n(i, j, t)$ is convected to the cell $(i+\delta i, j)$ at time $t+\Delta t$, where $\delta i = v_x(j)\,\Delta t/\Delta x$. The new density is simply $n(i+\delta i, j, t+\Delta t) = n(i, j, t)$.

When the number of cells crossed, $\delta x/\Delta x$, is not an integer, the particles are spread between two cells. If $\delta x/\Delta x = \delta i + \zeta$, where $0 \leqslant \zeta < 1$, then a fraction ζ of the particles represented by $n(i, j, t)$ are placed in the cell $(i+\delta i+1, j)$ and a fraction $(1-\zeta)$ and are placed in the cell $(i+\delta i, j)$, at the end of the time-step. The generalisation to a case where v_x changes during Δt is illustrated schematically in Fig. 1a for an arbitrary pair of independent variables (x, y), so y should be interpreted as v_x, and $\dot{y} \equiv \dot{v}_x$ in this example.

This procedure, which we shall refer to as a "convected scheme" (CS) reduces to an explicit finite difference scheme in the limit of very small time steps, i.e., time steps which obey the CFL criterion. In this case, $\delta i = 0$ and typically $\zeta \ll 1$. To see how the finite difference result is recovered, note that a fraction of the particles represented by $n(i, j)$ have flowed to $(i+1, j)$ in Δt. That fraction is $\zeta = \delta x/\Delta x = v_x(j)\,\Delta t/\Delta x$, so the total density at (i, j) is decreased by $n(i, j, t)\,v_x(j)\,\Delta t/\Delta x$, but added to by an amount $n(i-1, j, t)\,v_x(j)\,\Delta t/\Delta x$. Then the new density is

$$n(i, j, t+\Delta t) = n(i, j, t) + \left[\frac{n(i-1, j, t) - n(i, j, t)}{\Delta x}\right] v_x(j)\,\Delta t \tag{1}$$

which is the appropriate finite-difference equation. As we shall see below, this is a simple "upwind" scheme [6].

The effect of collisions is to further redistribute particles during the time step. This is handled in an intuitively appealing fashion by means of "propagators," which are the Green's functions for the short-time evolution of the distribution. The expressions given above are probably the simplest examples of propagators. The propagator $p(x, v_x, x', v_x', \Delta t)$ represents the probability of moving from (x', v_x') to (x, v_x) in a time Δt. In terms of the mesh labels, $p(i, j, i', j', \Delta t)$ is the probability of moving from the cell (i', j') to the cell (i, j) in time Δt. Then the new densities are given by

$$n(k, l, t+\Delta t) = \sum_{q, r} n(q, r, t)\, p(k, l, q, r, \Delta t). \tag{2}$$

In our previous example with no collisions, $p(k, l, k-\delta i, l, \Delta t) = 1-\zeta$, and $p(k, l, k-\delta i-1, l, \Delta t) = \zeta$, and all others are zero. Equation (2) thus reduces to Eq. (1) in this case provided that $\delta i = 0$ and $\zeta \ll 1$.

In practice it is not always convenient to implement the scheme in precisely the fashion implied by Eq. (2). Instead of evaluating all the contributions to the density arriving at a given point (the "postpoint") we actually concentrate on a single "prepoint" until we have determined the fate of all the fluid leaving that prepoint. This is important if the propagators must be normalized.

Charge exchange collisions will be treated in our example, and most other collision processes can be handled in a similar fashion. Coulomb collisions are discussed in the Appendix, but are ignored elsewhere in this paper.

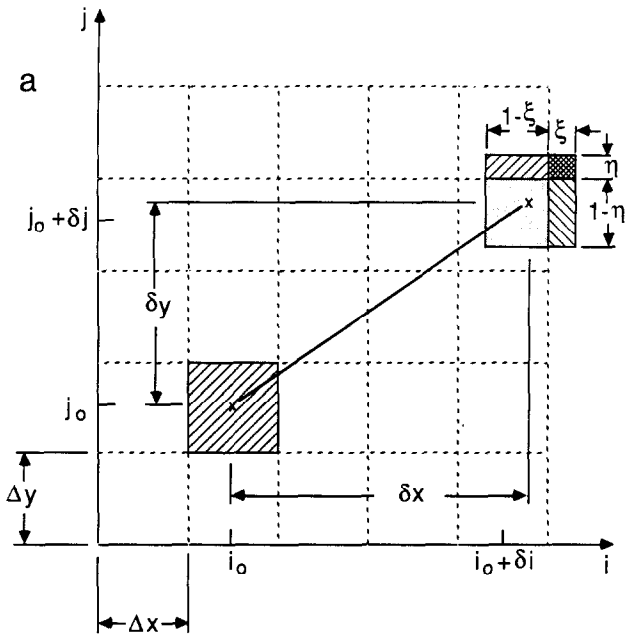

$$\delta x = (\delta i + \xi)\,\Delta x = \dot{x}\Delta t;\ 0 \leq \xi < 1$$

$$\delta y = (\delta j + \eta)\,\Delta y = \dot{y}\Delta t;\ 0 \leq \eta < 1.$$

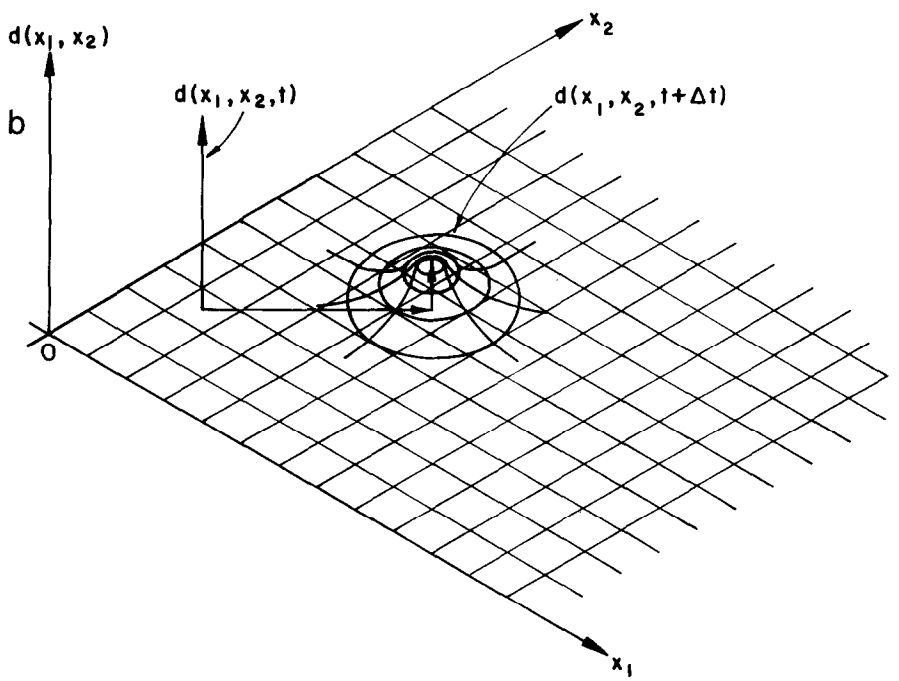

In a general collision process, particles are scattered into a wide range of final velocities. We break the propagator into two parts, one representing the unscattered particles and one representing the scattered particles. Since the number of unscattered particles decays exponentially, we can calculate the contribution of unscattered particles for the case where $v_x = \text{constant}$ and the mean-free-path is $\lambda(v_x)$. For propagation from the prepoint at (k, l) we have the contribution of unscattered particles

$$p(k+\delta i, l, k, l, \Delta t) = (1-\zeta)\, e^{-\delta x/\lambda(l)} \tag{3a}$$

to the postpoint $(k+\delta i, l)$ and, similarly,

$$p(k+\delta i+1, l, k, l, \Delta t) = \zeta e^{-\delta x/\lambda(l)} \tag{3b}$$

at the postpoint $(k+\delta i+1, l)$; there is no contribution from unscattered particles, elsewhere. An expression such as this allows a large time-step, provided $\lambda \gg \Delta x$, which illustrates the sense in which convection must predominate over diffusion.

There is also a contribution from those particles which did undergo collisions and which have been redistributed in v_x in an as-yet unspecified fashion. Since collisions took place all the way from cell k to the cell $(k+\delta i+1)$, the particles lost will in general be spread out in the same spatial range.

An illustration of calculating the new velocity of scattered particles can be given for charge exchange collisions which result in new ions at the neutral temperature, T_n. In the example considered in Section III, $T_n = 300\ K$, and the collisions result in a reduction of the velocity to essentially zero, so those particles which are scattered have their velocity set to $v_x = \pm \Delta v/2$, that is, they are added to the corresponding cell of the mesh at the spatial position where the collision occurred, which was in the range k to $k+\delta i+1$. (Our mesh straddles the $v_x = 0$ axis. The number of spaces in v_x is N_v and the point $N_v/2$ is at $-\Delta v/2$; the point at $N_v/2+1$ is at $+\Delta v/2$.)

In the light of all this, we shall now give an explicit description of the fate of the particles initially in a cell (i_0, j_0), for general velocities and accelerations and subject to charge-exchange collisions with cold neutrals (the case treated here). In doing so, we shall point out the limitations of the approach. The treatment of the equations of fluid transport using propagators is discussed in the Appendix.

FIG. 1. (a) The simplest "convected scheme," with constant flow velocities in x and y. A histogram is convected from its initial cell and redistributed amongst four "final" cells. In this paper, we use the independent variables (x, v_x) so $y \equiv v_x$ and $\dot{y}$ is the acceleration $\dot{v}_x$. (b) The propagator for diffusion in the presence of flow, based on a displaced Gaussian. A delta-function distribution, denoted by the vertical arrow on the left, flows to the position of the vertical arrow on the right, due to convection, and spreads out into a Gaussian, due to diffusion.

TABLE I

Flow Chart of Numerical Method

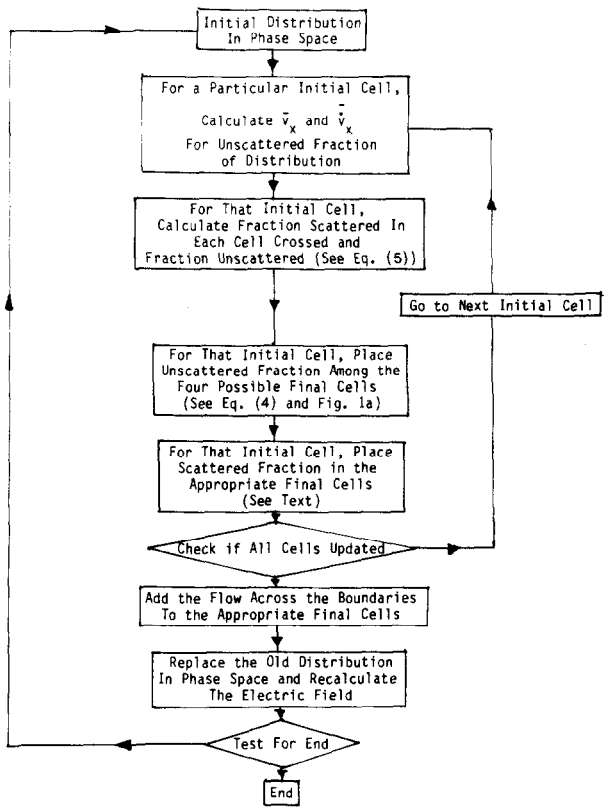

B. *Description of the General Numerical Method*

We now explain the method in detail, for a realistic case, including acceleration and collisions (see also the flow chart in Table I). We begin by finding the final position of the particles which start in the cell (i_0, j_0) and which do not undergo collisions. The initial (x, v_x) corresponding to (i_0, j_0) are known, and the initial $\dot{v}_x$ is found from the initial position (since the force, given in this case by $E_x(x)$, the electric field, is known). The final (x, v_x) are found to the desired accuracy by a Runge–Kutta scheme or similar method. In effect, the Runge–Kutta scheme establishes appropriate averages along the computed trajectory of the velocity $\bar{v}_x$ and the acceleration $\bar{\dot{v}}_x$, $\tau\bar{v}_x = \int v_x\, dt$, and $\tau\bar{\dot{v}}_x = \int \dot{v}_x\, dt$. (As we shall see below, intermediate values of (x, v_x) are also required and these are also obtained from the Runge–Kutta scheme.) In terms of Fig. 1a we use $\dot{x} \equiv \bar{v}_x$ and $\dot{y} \equiv \bar{\dot{v}}_x$ (since y corresponds to v_x).

The unscattered portion of the histogram can then be distributed amongst the four final cells, as illustrated in Fig. 1a, once the number scattered is known. The unscattered fraction is divided amongst the four final cells, with the fractions of f_{uns} being distributed as

$$\begin{array}{lll} (1-\zeta)(1-\eta) & \text{in cell} & (i_0+\delta i,\, j_0+\delta j) \\ (1-\zeta)\eta & \text{in} & (i_0+\delta i,\, j_0+\delta j+1) \\ \zeta(1-\eta) & \text{in} & (i_0+\delta i+1,\, j_0+\delta j) \\ \zeta\eta & \text{in} & (i_0+\delta i+1,\, j_0+\delta j+1). \end{array} \tag{4}$$

The next problem is to find the fraction of the histogram which is scattered, each time a spatial mesh-spacing Δx is crossed. The velocities found previously from the Runge–Kutta scheme at various points on the trajectory are used to estimate $\lambda(v_x)$ along the trajectory. A fraction of the (remaining) particles $(1-e^{-\Delta x/\lambda(v_x)})$ is scattered in each cell crossed. These are divided between $v_x=+\Delta v/2$ and $v_x=-\Delta v/2$, i.e., on either side of $v_x=0$ (since the ions produced by charge exchange are considered to be "cold"), at the spatial position at which they were scattered, and the unscattered particles are handled as described above.

As a result of this, the fraction of particles which are not scattered is

$$f_{\text{uns}}=e^{-\delta x/\bar{\lambda}}. \tag{5}$$

$\bar{\lambda}$ is an appropriate average of the mean-free-path, such that

$$\frac{\delta x}{\bar{\lambda}}=\frac{\Delta x}{\lambda_1}+\frac{\Delta x}{\lambda_2}+\cdots+\frac{\Delta x}{\lambda_{\delta i}}+\frac{\zeta\Delta x}{\lambda_{\delta i+1}}, \tag{6}$$

where $\lambda_1=\lambda(v_{x1})$ and v_{x1} is the velocity in the first cell crossed, etc. (In practice, λ will be essentially the same in many of the cells crossed.)

Next, the flow of particles across the boundary into the region must be accounted for; this is discussed below in Section C. Finally, the electric field is recalculated. This completes the procedures involved in advancing through a time-step, and we will now discuss two issues related to the efficiency and accuracy of the method.

The Runge–Kutta procedure is not necessary at low velocities since all the information needed to describe the step (intermediate and final values of (x, v_x)) can be obtained sufficiently accurately without resort to the Runge–Kutta, provided the electric field is not very strong. At higher velocities typically only a low-order scheme is necessary. If greater accuracy is necessary, this is an indication that the electric field is strong enough to warrant a reduced time-step. The need for a Runge–Kutta scheme reduces the efficiency by a factor $\lesssim 2$ relative to what might be expected on the basis of the time-step, since it leads to a duplication of a portion of the operations involved in taking a step.

When particles are replaced at low velocities after they undergo a collision, their subsequent motion during the time-step in which they were scattered is neglected. This is not necessary, but was convenient in this case. For most cases this is a reasonable assumption, as explained below.

If $v\Delta t \ll \lambda$ for the bulk distribution, then few scattered particles are created, so the error is small. Since λ typically increases with energy, for energies of several tens of electron volts, this is often the case. If the scattered particles travel a distance $v\Delta t$ which is much less than a scale length L_s, on which conditions vary, there is no substantial error, since those flowing out of a given cell are replaced by similar particles. (If $v\Delta t$ is less than a mesh spacing Δx there is no error, but presumably $\Delta x < L_s$.) Finally, if $\Delta t \ll T$, the typical time-scale on which the system varies, the method is accurate, since in the limit T is very large the scattering is performed on what is essentially a steady-state distribution and so the time when the scatter occurs is not critical. These last two statements are similar, in that we expect $L_s = vT$, in many cases. If all of these conditions fail, then the system is not well resolved, either spatially or temporally, and Δt must be reduced. This would be true however we handle the collision processes, since if $\Delta t \sim T$, we cannot follow the evolution satisfactorily.

C. *Boundary Conditions*

The boundary conditions for the kinetic problem are straightforward; ions flow into the solution region at $x = 0$, $v_x \geqslant 0$ (see Figs. 3–6). Their distribution at $x \leqslant 0$ (i.e., the particles which are flowing into the solution region) is specified externally. Any particles leaving at the edges in x, i.e., at $x = 0$ and $x = L$, are allowed to do so. The density near the boundaries in v_x is negligible, so no particles leave at these edges.

The ion flux in through the boundary must be handled separately from the main integration. We take the density at $x = 0$ and propagate it forward during a time-step; however, it is also necessary to consider those particles from $x < 0$ which enter the solution region in that time. Otherwise too few particles enter (and those that do, arrive in "clumps"). We achieve this by taking the density at $x = 0$ and propagating it through $\tau < \Delta t$. We then add this to the density which arrived at $x = 0$ in this time (i.e., the same density as before) and repeat the procedure, propagating the total density so created forward. The ion "injection" is thus described by a boundary term, which in general can be constructed using expressions (4)–(6), with a sequence of N short time-steps of length τ such that $N\tau = \Delta t$, the step used in the main integration, and with a finer mesh than used ordinarily. This contribution to the density represents the ions which flow into the region being described during one time-step Δt, and so must be added to the density after each time-step.

D. *Discussion of the Numerical Method*

This method for following the time evolution of the density is straight-forward and intuitive to implement and very efficient. The increase in efficiency, however, is

entirely dependent on the application; our specific example has an increase in speed $\simeq \Delta t/\Delta t_{\mathrm{CFL}}$ (assuming it takes as long to take a step by each method) and this is over 100 in the case we examine in Section III, at all but the highest collision frequencies. The limit on Δt could be set by the collision time (as mentioned above) or we may choose Δt to preserve accuracy in calculating the position in phase space to which the fluid flows. The method is extendable to arbitrary numbers of dimensions, with no additional difficulty in encoding.

The CS was developed so as to combine the flexibility of Monte Carlo methods with the more complete description of the density provided by a finite difference scheme. Calculations which are essentially Monte Carlo (or "particle") methods but which in some sense provide a solution of the diffusion equation have been investigated in detail [9]. The distinction between those methods and the present work is essentially that we obtain solutions on a grid. The particle method is subject to statistical fluctuations which are not evident in a grid-based method.

The numerical scheme which is closest in its intent to the CS is probably upstream (or upwind) differencing [6, 10]. It provides a solution on a mesh, by making use of the physical nature of the flows. A very simple upstream differencing scheme is given in Ref. [6]; for the equation

$$\frac{\partial n}{\partial t} + a\frac{\partial n}{\partial x} = 0, \qquad a = \text{const} > 0.$$

This is represented as

$$n(x, t+\Delta t) = n(x, t) - \lambda a(n(x, t) - n(x-\Delta, t))$$

(in our notation). This is identical to Eq. (1), when λ is written appropriately; in other words, the CS reduces to an upwind scheme in the limit of small Δt. This scheme is subject to the CFL criterion [6] $\lambda a \leqslant 1$. Several explicit upstream schemes are discussed in Ref. [6]. The CS differs from these in that it does not obey a CFL criterion, since it does not rely on (explicit or implicit) finite differences. The failure of the accuracy of an implicit upwind scheme in a (stationary) flow/diffusion problem has been discussed by Arter [10].

The CS advocated here is in one sense mathematically well known, since it essentially consists of performing a convolution integral. In the language of systems analysis, the propagator is an "impulse response." The "signal" $n(x, v_x, t)$ is the input and the "output" is $n(x, v_x, t+\Delta t)$. The "system" which converts input to output and to which the impulse response refers consists of the phase-space trajectories of particles during the time Δt. Contrary to most systems applications, the convolution is over the phase space, S, instead of time (see Fig. 2):

$$n(x, v_x, t+\Delta t) = \int n(x', v_x', t)\, p(x, v_x, x', v_x', \Delta t)\, dS'. \tag{7}$$

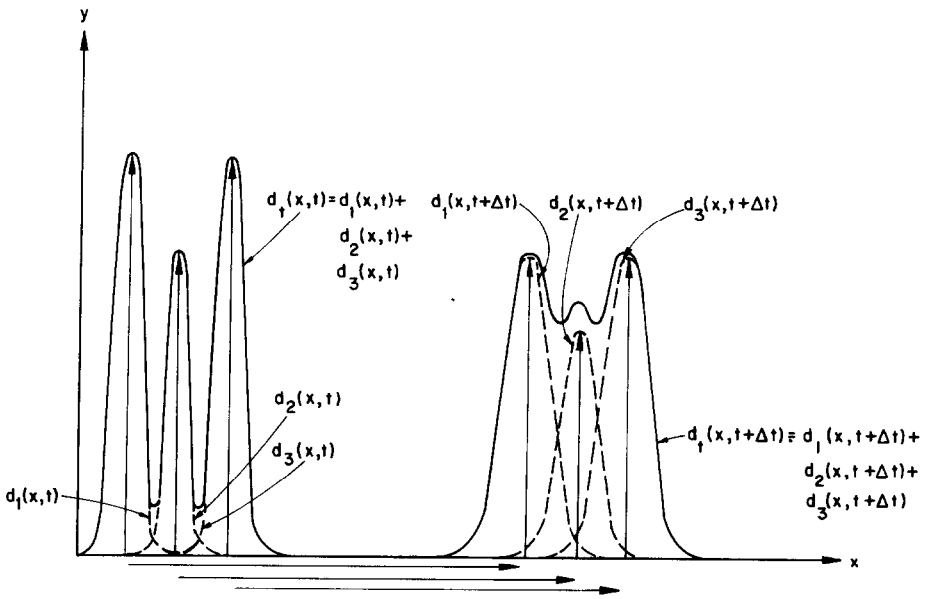

FIG. 2. Calculation of the time evolution of the distribution.

Although numerical convolution is occasionally performed directly, it is usually for pedagogical purposes. Efficient evaluation tends to be performed by multiplication of the appropriate Fourier transformed quantities [11]. Fourier transforms are not convenient in this case; the back-transform in particular would be cumbersome to perform.

The link to general methods of solution of integral equations and Green's function methods is also clear. The essential point of the CS is that it is a numerical realisation of Eq. (7) which exploits the full potential of the integral equation for problems where a suitable Green's function can be found; in this paper our focus is on transport problems where convection is in some sense dominant. We are aware of no previous work (except our own preliminary study, Ref. [4]) pointing out how such an approach should be implemented, as we are attempting to do here.

III. ION DISTRIBUTION IN A PLASMA SHEATH

In this section we consistently obtain the ion distribution and the electrostatic potential in a plasma sheath, using as a boundary condition the distribution functions at the boundary between the sheath and the rest of the plasma obtained

by Emmert *et al.* [12]. The plasma sheath is a region at the edge of a plasma where the plasma comes in contact with a material boundary. Under most circumstances, the steady-state fluxes of ions and electrons to this boundary must be (roughly) equal to prevent the buildup of charge. The fluxes are normally made equal because the electron flux initially exceeds the ion flux until a negative charge sufficient to repel most electrons builds up on the plate (or boundary). The sheath is thus a region of strong electric fields from which the main plasma is shielded by the mobile electrons. The fields decay spatially on a scale set by the Debye length, λ_D, as a result of this shielding.

The electric fields in the sheath thus accelerate ions to the plate (where we shall assume they are neutralised) and repel electrons. The electrons are nearly all reflected and confined to the plasma region, and so their density may be assumed to obey a Boltzman relation, $n_e = n_{e0} e^{q\Phi/kT}$. The calculation of the ion distribution function is then the main problem, and this must be done consistently with the electrostatic potential set up.

Most treatments of the sheath assume the sheath length to be zero or so short that it is essentially collisionless. Bohm [13] found the minimum kinetic energy for cold ions entering a sheath of non-zero length which was consistent with a monotonic potential, assuming a Boltzmann distribution for the electrons. A more complex set of assumptions was examined by Riemann [14], who used a two-scale analysis for the plasma and the sheath respectively. Riemann assumed $T_i \ll T_e$, a constant mean-free path, λ, for charge exchange interactions and $\lambda \gg \lambda_D$, the Debye length, and found an analytic expression for the sheath potential drop that was contingent upon finding the ion distribution function at the plasma–sheath interface. (In this work, we use the distribution function found by Emmert *et al.* [12] for ions flowing into the sheath, as stated above.)

The explicit evaluation of the distribution function usually necessitates a numerical solution. Computer programs which find the distribution in a given field (see, e.g., Ref. [3]), have been developed, although the field is not evaluated consistently with the distribution. The case of a mono-energetic beam has been treated consistently by Whealton [15].

The kinetic equation for the distribution function is

$$\frac{\partial f}{\partial t} + v_x \frac{\partial f}{\partial x} + \dot{v}_x \frac{\partial f}{\partial v_x} = C(f), \tag{8}$$

where f is the ion distribution function in (x, v_x). The propagator used is that described in the previous section. The exponential decay in Eq. (4) corresponds to the effect of the negative term in a collision operator $C(f) \equiv (f_M - f)/\tau$, where $\tau \equiv \lambda(v_x)/v_x$ and f_M is a Maxwellian, such that $n(x) \equiv \int f \, dv_x = \int f_M \, dv_x$. Physically, this represents the charge-exchange collisions of ions with neutral atoms. The negative term $-f/\tau$ is the rate at which ions are removed, and the positive term (which gives an equal rate when integrated over v_x) is the rate of production of new

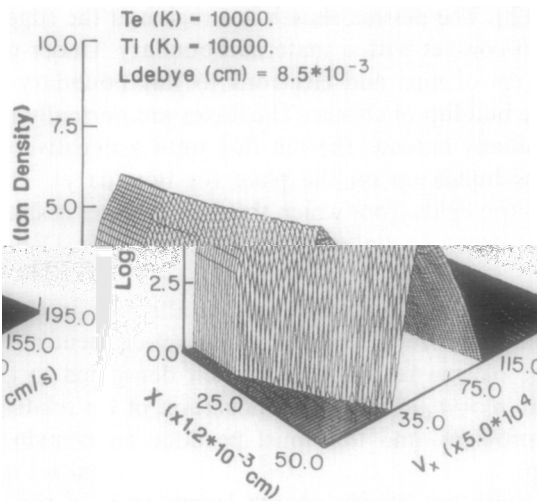

FIG. 3. Ion distribution function, for $T_i = T_e = 1$ eV, $\lambda_D = 8.5 \times 10^{-3}$ cm, $n_n = 0$ plotted vs. (x, v_x). The plot shows $\log_{10} f_i$.

ions, at the neutral temperature. The net result of collisions is to redistribute ions in v_x, leaving x unchanged.

Our method essentially allows a very efficient self-consistent evaluation of the distribution function in the sheath and the potential profile across the sheath, which would otherwise have to be calculated using a finite-difference scheme. A typical mesh employed (100×100) mesh spaces, in the velocity and spatial ranges shown on the figures. The calculations were performed on the CRAY I, and took

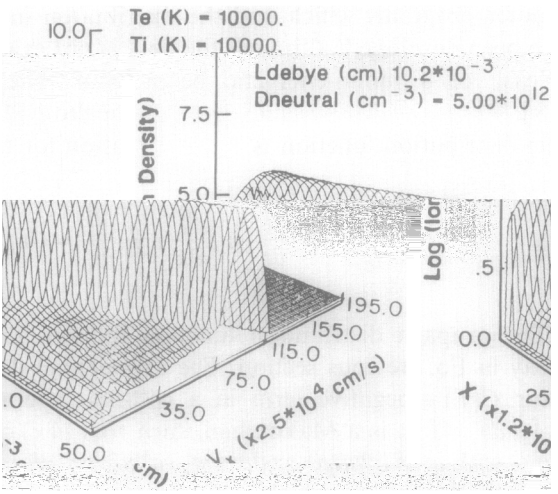

FIG. 4. As Fig. 3, with $n_n = 5 \times 10^{12}$ cm^{-3}, $\lambda_D = 1.02 \times 10^{-3}$ cm.

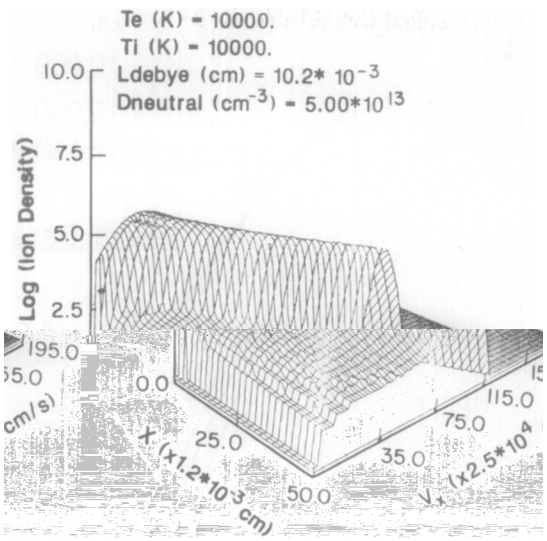

FIG. 5. As Fig. 4, with $n_n = 5 \times 10^{13}\ \mathrm{cm}^{-3}$.

5–10 CPU min for the electric field to converge (which was much slower than finding a solution for a given electric field).

The distribution for a collisionless ($n_n = 0$) case with $T_i = T_e = 1$ eV, is shown in Fig. 3. For a grid with 100 mesh spaces in the x direction, the potential drop which was obtained agrees to within 1% with the value predicted by Emmert *et al.* [12]. (See also Ref. [16].) This agreement illustrates that the CS is accurate.

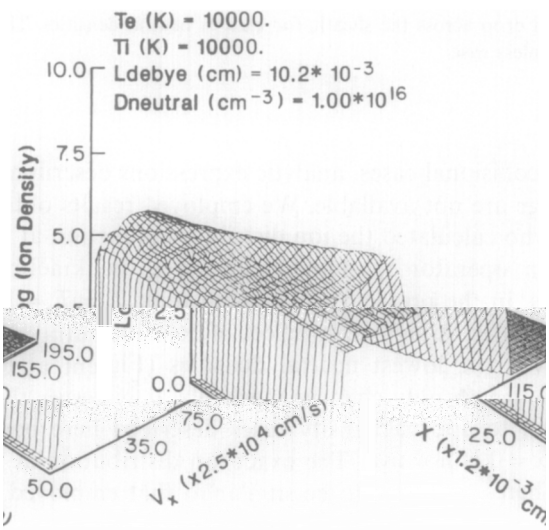

FIG. 6. As Fig. 4, with $n_n = 10^{16}\ \mathrm{cm}^{-3}$.

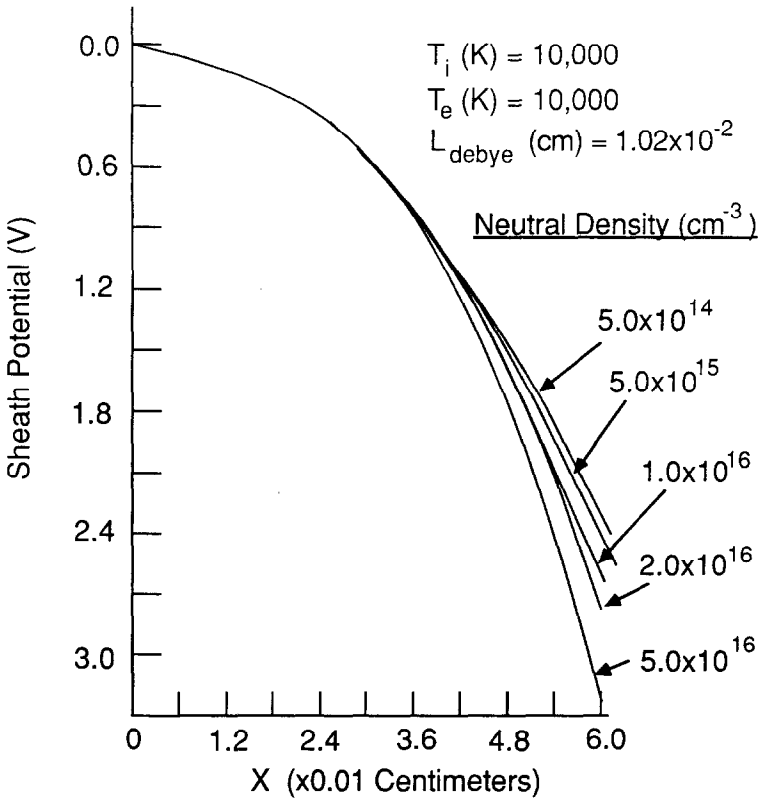

FIG. 7. Potential drop across the sheath, for various neutral densities. The lowest density shown is essentially a collisionless case.

For the most collisional cases, analytic expressions describing the ion distribution at the sheath edge are not available. We employed results obtained by Scheuer and Emmert [17], who calculated the ion distribution function at the sheath edge using a BGK collision operator to numerically solve the kinetic equation, including (weak) collisions, in the presheath. We again took $T_i = T_e = 1$ eV, but employed a wide range of neutral densities. A significant effect of collisions on the distribution function is evident at even the lowest neutral densities (Figs. 4–6) but the total potential drop across the sheath only changes markedly at high densities (Fig. 7).

The higher density cases described here begin to approach conditions in some glow discharges. The exact ion distribution at $x = 0$ is not available in these cases, but is expected to be similar to that employed here.

IV. Summary

An efficient numerical treatment of fluid transport in the presence of strong convective flow has been described. The method employs propagators, which are accurate for time steps which are prohibited by the CFL criterion in finite-difference schemes, to describe the flow and in addition to describe the effects of collision processes and diffusion. A step-by-step illustration of the implementation of the method was presented, and its mathematical foundations were discussed. Conditions were specified for which the CS is most efficient; in the example studied, the efficiency gain versus an explicit scheme is of the order of 100, provided individual steps take about as long in either method, which is approximately the case.

The method was applied to a problem in two independent variables, the kinetic treatment of the plasma sheath, in variables (x, v_x). The sheath calculation was performed for a wide range of neutral densities, using an energy-dependent collision cross section for ion-neutral collisions, and was shown to yield accurate results in the case where collisions were absent.

Appendix

In the discussion in the main body of the paper, the independent variables were (x, v_x). However, the method is equally applicable in other independent variables, such as purely spatial variables (x, y). (The number of independent variables is also easily extended.) In this case, the flux of particles is usually a combination of a convective term and a diffusive term;

$$\Gamma = n\mathbf{v} - D\,\nabla n. \tag{A1}$$

The equation of conservation of particles can then be written as

$$\frac{\partial n}{\partial t} + \nabla \cdot (n\mathbf{v}) - \nabla \cdot (D\,\nabla n) = S, \tag{A2}$$

where S is the rate of production of particles, per unit volume. The velocity $\mathbf{v}$ and diffusion coefficient D are assumed known, in this discussion.

To emphasize its generality, we now write the propagator for this equation in terms of independent variables (x_1, x_2). This is the solution of Eq. (A2) in an unbounded region when the initial distribution was a delta function at (x_{10}, x_{20}),

$$p(\mathbf{x}, \mathbf{x}_0, \Delta t) = \frac{1}{2\pi\,\Delta t\,\sqrt{D_{11}D_{22}}} \exp\left\{-\left(\frac{(x_1 - x_{10} - v_1\,\Delta t)^2}{2D_{11}\,\Delta t} + \frac{(x_2 - x_{20} - v_2\,\Delta t)^2}{2D_{22}\,\Delta t}\right)\right\} \tag{A3}$$

for a diagonal diffusion tensor such that $D_{12} = D_{21} = 0$ (Fig. 1b). This expression is a Gaussian centred on $(x_{10} + v_1 \Delta t, x_{20} + v_2 \Delta t)$, which is the solution of Eq. (A2) in the circumstances indicated above. Here $v_1 \equiv \dot{x}_1(\mathbf{x})$, $v_2 \equiv \dot{x}_2(\mathbf{x})$, where $\dot{x} \equiv dx/dt$. v_1 and v_2 are typically obtained at the start of the step, but can be found by interpolation, as discussed above. If $\mathbf{v}$ or D are not constant, Eq. (A3) is only approximate, and the step is limited to the region where they are almost constant. In the phase space (x, v_x), x_2 is $\dot{x}_1$, so v_2 is $\ddot{x}_1$. The summation of terms (Eq. (2) or Eq. (7)) using Eq. (A3) is illustrated in Fig. 2.

In highly ionised plasmas, collisions are predominantly Coulomb collisions, and so diffusion takes place in v_x; there is no spatial diffusion term in the kinetic equation, so $D_{11} = 0$ and the propagator in the (x, v_x) phase space becomes

$$p(x, v_x, x_0, v_{x0}, \Delta t) = \frac{\delta(x - x_0 - v_x \Delta t)}{\sqrt{2\pi D_{vv} \Delta t}} \exp\left(\frac{-(v_x - v_{x0} - \dot{v}_x \Delta t)^2}{2D_{vv} \Delta t}\right). \quad \text{(A4)}$$

This describes a flow in x, from x_0 to $x_0 + v_x \Delta t$; in v_x there is a flow to the point $v_{x0} + \dot{v}_x \Delta t$ and diffusion gives rise to a broadening, so this point is the centre of the Gaussian.

Highly ionised plasmas are often "convection dominated," and so the CS offers significant advantages over conventional numerical solutions of the kinetic equation [7, 8].

ACKNOWLEDGMENTS

We thank T. J. Sommerer, A. Thyagaraja, and J. W. Eastwood for their comments and clarifications of this manuscript.

REFERENCES

1. D. POTTER, *Computational Physics* (Wiley, New York, 1973).
2. W. H. PRESS, B. P. FLANNERY, S. A. TEUKOLSKY, AND W. T. VETTERLING, *Numerical Recipes: The Art of Scientific Computing* (Cambridge Univ. Press, Cambridge, 1986).
3. W. L. MORGAN, Joint Inst. Lab. Astrophys. Inform. Center, Boulder, CO, Report 19, 1979 (unpublished).
4. J. B. ADAMS AND W. N. G. HITCHON, *J. Comput. Phys.* **76**, 159 (1988).
5 M. F. WEHNER AND W. G. WOLFER, *Phys. Rev. A* **27**, 2663 (1983).
6. A. HARTEN, P. D. LAX, AND B. VAN LEER, *SIAM Rev.* **25**, 35 (1983).
7. S. P. HIRSHMAN, K. C. SHAING, W. I. VAN RIJ, C. O. BEASLEY, AND E. C. CRUME, *Phys. Fluids* **29**, 2951 (1986).
8. H. E. MYNICK AND W. N. G. HITCHON, *Nucl. Fusion* **26**, 425 (1986).
9. A. F. GHONIEM AND F. S. SHERMAN, *J. Comput. Phys.* **61**, 1 (1985).
10. W. ARTER, Culham Report CLM-P835, January 1988; *J. Comput. Phys.*, in press.
11. H. D. REES, *J. Phys. Chem. Solids* **30**, 643 (1969).

12. G. A. EMMERT, R. M. WIELAND, A. T. MENSE, AND J. M. DAVIDSON, *Phys. Fluids* **23**, 803 (1980).
13. D. BOHM, *The Characteristics of Electrical Discharges in Magnetic Fields*, edited by A. Guthrie and R. K. Wakerling, Eds. (McGraw–Hill, New York, 1949), Chap. 3.
14. K.-U. RIEMANN, *Phys. Fluids* **24**, 2163 (1981).
15. J. H. WHEALTON, *J. Comput. Phys.* **63**, 20 (1986).
16. R. C. BISSELL AND P. C. JOHNSON, *Phys. Fluids* **30**, 779 (1987).
17. J. T. SCHEUER AND G. A. EMMERT, *Phys. Fluids B* **31**, 1748 (1988).